ELSEVIER

Biochimica et Biophysica Acta 1540 (2001) 107–126

BIOCHIMICA ET BIOPHYSICA ACTA

BBA

www.bba-direct.com

Maitotoxin activates an endogenous non-selective cation channel and is an effective initiator of the activation of the heterologously expressed hTRPC-1 (transient receptor potential) non-selective cation channel in H4-IIE liver cells

Helen M. Brereton [a], Jinglong Chen [a], Grigori Rychkov [b], M. Lyn Harland [a], Gregory J. Barritt [a,*]

[a] *Department of Medical Biochemistry, School of Medicine, Flinders University, G.P.O. Box 2100, Adelaide, SA 5001, Australia*

[b] *Centre for Advanced Biomedical Studies, University of South Australia and Department of Physiology, University of Adelaide, G.P.O. Box 498, Adelaide, SA 5001, Australia*

Received 19 June 2000; received in revised form 28 May 2001; accepted 29 May 2001

Abstract

The structures and mechanisms of activation of non-selective cation channels (NSCCs) are not well understood although NSCCs play important roles in the regulation of metabolism, ion transport, cell volume and cell shape. It has been proposed that TRP (transient receptor potential) proteins are the molecular correlates of some NSCCs. Using fura-2 and patch-clamp recording, it was shown that the maitotoxin-activated cation channels in the H4-IIE rat liver cell line admit Ca^{2+}, Mn^{2+} and Na^{+}, have a high selectivity for Na^{+} compared with Ca^{2+}, and are inhibited by Gd^{3+} (half-maximal inhibition at 1 μM). Activation of the channels by maitotoxin was inhibited by increasing the extracellular Ca^{2+} concentration or by inclusion of 10 mM EGTA in the patch pipette. mRNA encoding TRP proteins 1, 2 and 3 at levels comparable with those in brain was detected using reverse transcriptase–polymerase chain reaction in poly(A)$^{+}$ RNA prepared from H4-IIE cells and freshly-isolated rat hepatocytes. In H4-IIE cells transiently transfected with cDNA encoding hTRPC-1, the expressed hTRPC-1 protein was chiefly located at intracellular sites and at the plasma membrane. Cells expressing hTRPC-1 exhibited a substantial enhancement of maitotoxin-initiated Ca^{2+} inflow and a modest enhancement of thapsigargin-initiated Ca^{2+} inflow (measured using fura-2) and no enhancement of the highly Ca^{2+}-selective store-operated Ca^{2+} current (measured using patch-clamp recording). In cells expressing hTRPC-1, maitotoxin activated channels which were not found in untransfected cells, have an approximately equal selectivity for Na^{+} and Ca^{2+}, and are inhibited by Gd^{3+} (half-maximal inhibition at 3 μM). It is concluded that in liver cells (i) maitotoxin initiates the activation of endogenous NSCCs with a high selectivity for Na^{+} compared with Ca^{2+}; (ii) TRP proteins 1, 2 and 3 are expressed; (iii) maitotoxin is an effective initiator of activation of heterologously expressed hTRPC-1 channels; and (iv) the endogenous TRP-1 protein is unlikely to be the molecular counterpart of the maitotoxin-activated NSCCs nor the highly Ca^{2+}-selective store-operated Ca^{2+} channels.

Keywords: H4-IIE cell; Patch-clamp recording; Reverse transcriptase–polymerase chain reaction; Ca^{2+}, Mn^{2+} and Na^{+} inflow; Heterologous expression; Gd^{3+}

Abbreviations: $[Ca^{2+}]_{cyt}$, the concentration of free Ca^{2+} in the cytoplasmic space; NSCC, intracellular messenger-activated non-selective cation channel; GFP, green fluorescent protein; GAPDH, glyceraldehyde 3-phosphate dehydrogenase; DMEM, Dulbecco's Modified Eagles Medium

* Corresponding author. Fax: +61-8-8374-0139. *E-mail address:* greg.barritt@flinders.edu.au (G.J. Barritt).

0167-4889/01/$ – see front matter
PII: S0167-4889(01)00124-0

1. Introduction

Freshly isolated rat hepatocytes and rat liver cell lines possess two main types of plasma membrane Ca^{2+} channels which are activated by the binding of a hormone or growth factor to its receptor on the plasma membrane. These are the Ca^{2+} selective store-operated Ca^{2+} channels (also called Ca^{2+} release-activated Ca^{2+} channels) the activation of which is initiated by a decrease in Ca^{2+} in the endoplasmic reticulum, and intracellular messenger-activated non-selective cation channels (NSCCs) (reviewed in [1–4]). The physiological functions of liver cell NSCCs are not well defined but may include the delivery of Ca^{2+} to specific regions of the cytoplasmic space, a contribution to the replenishment of Ca^{2+} in the endoplasmic reticulum, and the facilitation of Na^+ inflow. Subsequent changes in $[Ca^{2+}]_{cyt}$ and in the concentration of intracellular Na^+ may contribute to the regulation of liver cell metabolism, ion flow, cell volume and shape [1,5,6].

Several types of NSCCs have been identified in liver cells. These include channels activated by hormones, extracellular ATP, stretch, cyclic AMP (reviewed in [1–5]) and by the marine toxin, maitotoxin [7]. Maitotoxin, a polycyclic ether isolated from the marine dinoflagellate *Gambierdiscus toxicus*, activates NSCCs in many types of animal cells [7–13]. The mechanism(s) by which maitotoxin activates NSCCs is not well understood [11,13]. It most likely involves the binding of the toxin to a specific protein in the plasma membrane and the subsequent activation of an NSCC [13]. However, another possibility is that the hydrophobic polycyclic ethers moieties of maitotoxin are inserted into the plasma membrane to create a non-specific pore which admits Na^+ and Ca^{2+} to the cytoplasmic space [11]. It is proposed that either of these events, in turn, leads to depolarisation of the plasma membrane and an increase in $[Ca^{2+}]_{cyt}$; activation of voltage-operated Ca^{2+} channels (if present); activation of Ca^{2+}-dependent enzymes such as phospholipase C (which catalyses the formation of $Ins(1,4,5)P_3$); and the activation of NSCCs and other plasma membrane channels. Maitotoxin-induced increases in $[Ca^{2+}]_{cyt}$ and intracellular Na^+ concentration may also lead to the formation of arachidonic acid and other metabolites which may, under some conditions, mediate the formation of large cytolytic pores, additional inflow of ions and cell lysis [8,14].

The structures and mechanisms of activation of NSCCs are not well understood [6]. However, there is evidence that members of the TRP (transient receptor potential) family of proteins may be the molecular counterparts of some NSCCs [6,15,16]. The animal cell TRP proteins are homologues of the *Drosophila melanogaster* TRP and TRP-like (TRPL) proteins which form non-selective cation channels in the *Drosophila* photoreceptor cell (reviewed in [6,15,16]).

The aims of the present experiments were to elucidate the properties of the maitotoxin-activated NSCCs in liver cells using the H4-IIE rat liver cell line (derived from the Reuber hepatoma [3]), to investigate which TRP proteins are expressed in liver cells, and to test whether a TRP protein is the molecular counterpart of maitotoxin-activated NSCCs. The results indicate that maitotoxin initiates the activation of Gd^{3+} sensitive NSCCs which principally admit Na^+. Moreover, mRNA encoding each of the TRP proteins 1, 2 and 3 was detected in H4-IIE cells and in freshly isolated rat hepatocytes. Heterologous expression of the hTRPC-1 protein was found to be associated with a substantial enhancement of maitotoxin-stimulated Ca^{2+}, Mn^{2+}, and Na^+ inflow through channels which were not detected in control cells. It is concluded that maitotoxin initiates the activation of endogenous NSCCs, and is an effective initiator of the activation of the heterologously expressed hTRPC-1 protein, but that it is unlikely that the endogenous TRP-1 protein is the molecular counterpart of the endogenous maitotoxin-activated NSCCs.

2. Materials and methods

2.1. Materials

Maitotoxin was obtained from Sigma-Aldrich and cDNA encoding human (h)TRPC-1 in the expression vector pcDNA3 was kindly provided by Dr. C. Montell [17]. The sources of other reagents are as described below or previously [3,18].

2.2. Cell culture

The growth and sub-culture of H4-IIE cells (derived from a rat liver hepatoma) were performed as described previously [3,18]. AML12 mouse hepatocytes (ATCC CRL 2254), previously derived from mice transgenic for transforming growth factor α [19], were cultured at 37°C in 5% (v/v) CO_2 in air in Dulbecco's modified Eagle's medium (DMEM)/Ham's F12 nutrient mixture (Life Technologies) supplemented with 10% (v/v) foetal bovine serum, a mixture of insulin, transferrin and selenium (ITS) (Life Technologies), 0.1 μM dexamethasone, and 50 μg/ml gentamycin. H4-IIE and AML12 cells were subcultured for a maximum of 20 passages. Rat hepatocytes were isolated from rat liver by collagenase perfusion and grown in primary culture as described previously [18].

2.3. Molecular biology techniques

mRNA was prepared directly from rat hepatocytes (4×10^6 cells) grown overnight in primary culture, from cultured H4-IIE and AML12 cells (4×10^6 cells), and from freshly isolated rat brain (200 mg) using Oligo $(dT)_{25}$ magnetic beads (1 mg) (Dynal AS, Oslo, Norway) according to the manufacturer's instructions [20].

First-strand cDNA synthesis was conducted at 42°C for 75 min using 1 μg mRNA in a reaction mixture (25 μl total volume) which contained 200 units of Superscript II reverse transcriptase (RT), 40 units of RNase inhibitor, 1 mM dNTPs, 8.6 pmol oligo$(dT)_{17}$ adaptor primer, 10 mM dithiothreitol, 50 mM Tris–HCl (pH 8.0), 75 mM KCl and 3 mM $MgCl_2$ [21]. Amplification of cDNA (2-μl aliquots) was carried out in a reaction mixture (25 μl total volume) which contained 100 μM dNTP, 2 mM $MgCl_2$, 0.3 μM of each primer (except for the degenerate primer MTA which was used at 1 μM) and 0.6 units of Taq DNA polymerase. Reactions were incubated for 30 s at 94°C, 30 s at 55°C and 1 min at 72°C, for 45 cycles. Polymerase chain reaction (PCR) products were size-fractionated on 1.5% agarose gel and visualised by staining with ethidium bromide.

In order to amplify cDNA encoding TRP proteins 1–6, a common 8-fold degenerate antisense primer was employed. This was based on the highly conserved sequence in the predicted cytoplasmic region which is located next to the 3′ end of the sixth transmembrane segment in the *Drosophila* TRP and TRPL, human (h) TRP-1, and mouse (m) TRP-4 sequences [22–25]. Six specific sense primers (corresponding to TRP-1 to TRP-6) were based on the sequences of the mTRP fragments identified by Petersen et al. [25] and Zhu et al. [26]. Each sense primer was used in conjunction with the common antisense primer. The quality of the cDNA synthesised from each mRNA preparation was assessed by amplification using primers specific for glyceraldehyde 3-phosphate dehydrogenase [27]. The primer sequences and expected sizes of the PCR products are listed in Table 1.

The relative abundance of a given cDNA transcript obtained from different cell types was estimated by a strategy of limiting dilution PCR [18]. After synthesis of the cDNA, an aliquot of the reaction mixture was serially diluted in the range 1:5 to 1:100 000 and amplified as described above. The dilutions shown in Table 4 are the highest dilution from which it was possible to amplify PCR product that could be detected by ethidium bromide staining of the agarose gel. This limiting dilution procedure allows comparisons to be made between amplifications obtained from different cell types using the same primer set and conditions. However, it does not allow comparisons to be made between PCR products amplified using different primer sets.

For DNA sequencing, individual bands of PCR product were excised from the 1.5% agarose gel and the recovered DNA sequenced directly [21]. For confirmation of the sequence, all cDNA species were prepared at least twice using different cell preparations. All sequence data were obtained using the DyeDeoxy^T Terminator Cycle Sequencing kit and the 373A automated DNA sequencer (Applied Biosystems, Prism, CA). Sequence comparisons were performed with MacVector software, Version 5 (Oxford Molecular Inc., MD).

2.4. Transfection of H4-IIE cells with cDNA encoding green fluorescent protein and hTRPC-1

Cells were co-transfected [21] with cDNA encoding hTRPC-1 plus pEGFP-C1 (Clontech), which con-

Table 1
Sequences of the primers used for the detection by RT–PCR of mRNA encoding TRP proteins and glyceraldehyde 3-phosphate dehydrogenase (GAPDH) in rat brain, rat hepatocytes and liver cell lines

Primer[a]	Sequence	Expected size of PCR products (bp)	GenBank accession no.	Ref.
MTS 1 (TRP-1 sense)	ATG GGA CAG ATG TTA CAA	400	U40980 (mTRP-1)	[26]
MTS 2B (TRP-2 sense)	CGC TGG GCA CTC TGC AGA	370	U40981 (mTRP-2)	[26]
MTS 3 (TRP-3 sense)	AGG ACA TAT TCA AGT TCA	340	U40982 (mTRP-3)	[26]
MTS 4 (TRP-4 sense)	CAG ATA TCT CTG GGA AGG ATG	400	X90697 (mTRP-4)	[25]
MTS 5 (TRP-5 sense)	TTC TCT TTA TCT ACT GCC	360	U40984 (mTRP-5)	[26]
MTS 6 (TRP-6 sense)	TTC ATG GTC ATA TTC ATC	320	U49069 (mTRP-6)	[26]
MTA (common degenerate antisense)	TGG AGC RAA YTT CCA YTC[b]		J04844 (dTRP)	[22]
			M88185 (dTRPL)	[23]
			X90697 (mTRP-4)	[25]
			U31110 (hTRP-1)	[24]
GAPDH: sense	ACC ACA GTC CAT GCC ATC AC	450	M17701 (rGAPDH)	[27]
GAPDH: antisense	TCC ACC ACC CTG TTG CTG TA			

[a]MTS, mouse TRP sense primer; MTA, mouse TRP antisense primer. Each TRP sense primer (MTS) was used in conjunction with the common degenerate antisense primer MTA.
[b]R = G or A; Y = C or T.

tains cDNA encoding an enhanced green fluorescent protein (EGFP). This allowed the selection of transfected cells on the basis of their expression of GFP. Control cells were transfected with either pEGFP-C1 alone or with pEGFP-C1 plus the empty pcDNA3 vector lacking the hTRPC-1 cDNA. Cells were transfected using Fugene-6 transfection reagent (Roche Diagnostics Australia, NSW, Australia) according to the manufacturer's protocol. Cells (2×10^5) were suspended in 0.5 ml of antibiotic-free DMEM, treated with a mixture containing 3 μg hTRPC-1 cDNA, 0.3 μg pEGFP-C1 and 6 μl of Fugene-6 in serum- and antibiotic-free DMEM, and plated onto a collagen-coated coverslip. After 6 h, a further 1.5 ml of antibiotic-free DMEM was added and the cells were cultured for a further 18–22 h to permit protein expression before measurement of the amount of expressed hTRPC-1 protein and cation inflow.

2.5. Antibody synthesis and purification, preparation of cell lysates and Western blot analysis

An anti-TRP-1 antibody against the peptide, CRDLLGFRTSKYAMFYPRN, which corresponds to the 18 amino acids at the carboxy terminus of the mouse (m), human (h), bovine (b), and *Xenopus laevis* TRP-1 proteins (GenBank U73625, U31110, AF012900, AF127031, respectively) was raised in rabbits and purified by affinity chromatography as described previously [28].

Whole-cell protein extracts were prepared as follows. H4-IIE cells (20×10^6 cells) were harvested by trypsinisation, washed twice with phosphate-buffered saline (PBS), suspended in Lysis Buffer (500 μl) which consisted of 50 mM Tris–HCl (pH 7.5), 1 mM EDTA, 10 μM leupeptin, 10 μM pepstatin, 100 μM phenylmethylsulphonyl fluoride, 1 mM β-mercaptoethanol, 1% (v/v) Triton X-100 and 0.1% (w/v) sodium dodecyl sulphate (SDS), and incubated for 30 min at 4°C. Cell debris was removed by centrifugation at $1000\times g$ for 5 min at 4°C and samples of the supernatant used for Western blot analysis. A crude cellular membrane fraction was prepared as described previously [28] using the Lysis Buffer described above except that Triton X-100 and SDS were omitted. H4-IIE cells were disrupted by homogenisation (Ultra-turrax, 30 s) followed by sonication (Branson B-12 Sonifier, microtip, 30 s) at 0°C. Cell debris was removed by centrifugation at $1000\times g$ for 5 min at 4°C. The resulting supernatant was then centrifuged at $50\,000\times g$ for 30 min at 4°C to yield crude membrane (the precipitate) and cytosolic (the supernatant) fractions. The membrane fraction was suspended in one tenth of the original volume of Lysis Buffer. The cytosolic fraction was concentrated using a Centricon-10 concentrator

(Amicon, MA). Protein concentrations were determined by the Bradford method [29].

For Western blot analysis, protein extracts (40 μg protein) were subjected to 9% SDS–polyacrylamide gel electrophoresis then transferred to a nitrocellulose membrane (Hybond C+) by semi-dry blotting (HorizBlot, Atto Corporation, Japan) [30]. The membranes were blocked for 1 h at room temperature with a solution composed of 20 mM Tris–HCl (pH 8), 500 mM NaCl and 0.1% (v/v) Tween-20 (TBS-T) which contained 5% (w/v) skim milk powder, then incubated with the anti-TRP-1 polyclonal antibody (1 μg/ml in TBS-T containing 3% (w/v) skim milk powder) for 16 h at 4°C, followed by four washes (5 min each) with TBS-T. The secondary antibody, anti-rabbit IgG-peroxidase conjugate (1:2000 dilution in TBS-T containing 3% v/v skim milk powder) was applied for 1 h at room temperature followed by four washes with TBS-T. Bound peroxidase was detected by enhanced chemiluminescence [31] (ECL, Western Blotting Detection Reagents, Amersham), according to the manufacturer's instructions, followed by exposure of the membrane to X-Omat Blue XB-1 film. Where indicated, the anti-TRP-1 antibody (1 μg/ml) was blocked before use by incubation with antigenic peptide (1 μg/ml) for 2 h at 4°C followed by centrifugation at $14\,000\times g$ for 10 min at 4°C in order to remove immune complexes.

The relative amount of expressed hTRPC-1 protein in H4-IIE cells was estimated from the intensity of the hTRPC-1 band (80 kDa) calculated by volume integration using the GS-700 Imaging Densitometer and Molecular Analyst Image Analysis Software (Bio-Rad Laboratories, CA). In order to account for variations in the amount of protein present on the membrane, the intensity values were normalised by expressing each band as a ratio of the intensity of a non-specific band ($\sim$50 kDa) (unrelated to TRP-1) which was detected by the anti-TRP-1 antibody but was not blocked by peptide.

2.6. Immunolocalisation of the hTRPC-1 protein expressed in H4-IIE cells

H4-IIE cells expressing hTRPC-1 and EGFP, grown on collagen-coated coverslips, were rinsed with PBS and fixed with 4% (w/v) paraformaldehyde in PBS for 30 min, rinsed with PBS, then permeabilised with 1% (v/v) Triton X-100 in PBS for 4 min at room temperature. Cells were again rinsed with PBS, blocked with 20% (w/v) foetal bovine serum in PBS for 1 h at room temperature, washed with PBS containing 0.1% (v/v) Tween-20 (PBS-T), and incubated for 2 h at room temperature with rabbit polyclonal anti-TRP-1 antibody diluted 2 μg/ml in PBS-T. The cells were then washed with PBS-T and incubated for 1 h at room temperature in the dark with the secondary antibody, Cy3-conjugated anti-rabbit IgG at 1:200 dilution in PBS-T. After washing four times in PBS-T, the coverslips were mounted on glass slides and viewed using an Olympus AX70 fluorescence microscope (40× objective lens) in conjunction with a Hamamatsu ORCA cooled CCD camera. The filter blocks employed were Chroma 31001 NB (excitation 470–490 nm, emission 515–545 nm) for EGFP, Chroma 31002 (excitation 515–550 nm, emission 575–615 nm) for Cy-3.

2.7. Measurement of rates of Ca^{2+} and Mn^{2+} inflow

Rates of Ca^{2+} and Mn^{2+} inflow to H4-IIE cells were estimated using intracellular fura-2. Cells suspended in complete DMEM were plated onto circular collagen-coated [3] glass coverslips (22 mm diameter, approximately 0.2×10^6 cells per coverslip) and incubated for 24 h at 37°C in an atmosphere of 5% (v/v) CO_2 in air in order to create a cell monolayer. The cells were loaded with fura-2 by incubation of the coverslip/H4-IIE cell monolayer with 10 μM fura-2 acetoxymethylester in the presence of pluronic F-127 acid (0.025% (v/v)) in DMEM containing bovine serum albumin (2% w/v) for 30 min at 37°C in 5% (v/v) CO_2 in air. In some experiments (where indicated), the incubation was performed for 1 h at room temperature. The coverslip/H4-IIE cell monolayer was then washed twice at 37°C in 116 mM NaCl, 4.6 mM KCl, 1.2 mM $MgSO_4$, 1.2 mM KH_2PO_4, 25 mM $NaHCO_3$, and 20 mM TES, adjusted to pH 7.4 with NaOH (modified Krebs–Henseleit buffer), and mounted in a temperature-controlled incubation chamber (Applied Imaging, UK) placed on the microscope stage. Modified Krebs–Henseleit buffer (with, or without, added Ca^{2+} as indicated in the legends to figures) (300 μl) was then added to the incubation chamber. In experi-

ments in which Mn^{2+} inflow was measured or in which Gd^{3+} was employed, the modified Krebs–Henseleit buffer was replaced by a simpler HEPES-buffered saline medium which was composed of 140 mM NaCl, 5 mM KCl, 1 mM $MgCl_2$, 10 mM D-glucose, 15 mM HEPES, and 1 mM $CaCl_2$ (pH adjusted to 7.4 at 37°C with NaOH).

Cell fluorescence was measured at 34°C using an inverted Nikon TMD-EF fluorescence microscope, a 20× objective lens or a 40× glycerol immersion objective lens, an intensified CCD camera (ISIS-3/S20, Photonic Science) and Axon Imaging Workbench (Version 2.2) software. For Ca^{2+}, excitation was at 340 and 380 nm and the ratio of fluorescence intensity at 340 and 380 nm was determined. For Mn^{2+}, an excitation wavelength of 360 nm was employed. A Nikon UV filter block was used to isolate emitted light. Neutral density filters (2.0, 2.3, 2.6 or 3.0, as required) were incorporated into the excitation light path in order to decrease photobleaching. Each coverslip provided data from 25–50 different cells with varying degrees of loading with fura-2. Cells which exhibited initial (basal) fluorescence values below 100 and above 250 fluorescence ratio units were excluded from subsequent analysis. For Ca^{2+} measurements, values of maximum (R_{max}) and minimum (R_{min}) fluorescence ratio were estimated at the end of each experiment by the addition of 10 μM ionomycin (in the presence of 5 mM Ca^{2+}) and 20 mM EGTA (in 0.15 M Tris, pH 8.7), respectively, and were converted to $[Ca^{2+}]_{cyt}$ [32] using a value of 224 nM for the K_d for the association of Ca^{2+} with fura-2 [1,32].

The location of fura-2 in the cytoplasmic space of H4-IIE cells was verified as follows. Fura-2-loaded cells were treated with digitonin (20 μM) to selectively disrupt the plasma membrane but not intracellular membranes [32]. This released 70–85% of the cell-associated fura-2, indicating that the dye was principally located in the cytoplasmic space. This conclusion was confirmed by inspection of the location of fura-2 fluorescence in images of fura-2-loaded H4-IIE cells (results not shown). The possibility that maitotoxin treatment increases the loss of fura-2 from the cytoplasmic space [8], which would influence the observed rate of Mn^{2+}-induced quench of intracellular fura-2, was tested as follows. H4-IIE cells loaded with fura-2 were incubated in the presence or absence of 600 pM maitotoxin and their fluorescence measured (excitation wavelength 360 nm) as a function of time for 20 min. Cells incubated in the presence or absence of maitotoxin exhibited a loss of 8 ± 1% ($n = 3$) and 5.7 ± 0.3% ($n = 6$) of the initial value of fluorescence (about 200 fluorescence units), respectively, during this time period. These results indicate that maitotoxin does not induce a significant loss of fura-2 from H4-IIE cells under the conditions employed for the measurement of Ca^{2+} and Mn^{2+} inflow.

In some experiments, Ca^{2+} and Mn^{2+} inflow was measured in cells co-transfected with DNA encoding EGFP and hTRPC-1 (or empty vector). Although there is a considerable difference between the peak excitation wavelengths for EGFP (488 nm) and fura-2 (340 and 380 nm), it was possible that light emitted from EGFP in cells loaded with fura-2 interferes with the measurement of $[Ca^{2+}]_{cyt}$ and Mn^{2+} inflow. To test this possibility, the fluorescence of cells expressing EGFP and of control cells (no EGFP) was measured at excitation wavelengths of 340 and 380 nm (Ca^{2+}) and 360 nm (Mn^{2+}) using different neutral density filters and different gain settings for the CCD camera. The results (not shown) indicate that under the conditions employed for the measurement of Ca^{2+} and Mn^{2+} inflow in this study (neutral density filters greater than 2 and camera settings which minimise background fluorescence), the fluorescence of EGFP makes a negligible contribution to the observed fura-2 fluorescence emission.

Rates of Ca^{2+} inflow and amounts of Ca^{2+} released from intracellular stores were estimated as described previously [3]. Rates of Mn^{2+} inflow were estimated from the maximum slope of plots of fluorescence as a function of time following the addition of Mn^{2+} to cells loaded with fura-2. Results shown in the figures are the mean values obtained for the number of cells indicated in one experiment, while those in the tables and text are the means ± S.E.M. of those obtained for the total number of cells and number of separate experiments indicated. Degrees of significance were determined using Student's *t*-test for unpaired or paired samples, as indicated.

2.8. Electrophysiology

Whole-cell patch clamping [33] was performed at room temperature using a computer-based patch-

clamp amplifier (EPC-9, HEKA Electronics, Germany) and PULSE software (HEKA Electronics). The usual bath solution contained (mM): NaCl, 140; CsCl, 4; $CaCl_2$, 2; $MgCl_2$, 2; and HEPES, 10; adjusted to pH 7.4 with NaOH. When the concentration of divalent cations was changed in the external solution the concentration of NaCl was changed accordingly on an iso-osmolar basis. Two internal (pipette) solutions with different Ca^{2+} buffering capacities were employed. A strong Ca^{2+} buffer internal solution contained (mM): Cs glutamate, 120; CsCl, 10; MgATP, 2; EGTA, 10; and HEPES, 10; adjusted to pH 7.2 with KOH. A weak Ca^{2+} buffer internal solution contained (mM): Cs glutamate, 120; CsCl, 10; MgATP, 2; EGTA, 1; $CaCl_2$ 1; and HEPES, 10; adjusted to pH 7.2 with KOH. The internal solutions were hypotonic compared with the external solution in order to prevent the activation of volume-regulated Cl^- channels [5]. Depletion of intracellular Ca^{2+} stores was achieved by intracellular perfusion with the strong Ca^{2+} buffer internal solution.

Patch pipettes were pulled from borosilicate glass coated with Sylgard and fire-polished: pipette resistance ranged between 2 and 4 MΩ. In order to monitor the development of the current, voltage ramps between −120 and +60 mV were applied every 2 s, starting immediately after achieving the whole-cell configuration. Early traces were used for leakage subtraction. Acquired currents were filtered at 2.7 kHz and sampled at 10 kHz. Traces presented in the figures were further digitally filtered at 1.5 kHz. All voltages shown are nominal voltages, and have not been corrected for the liquid junction potential of −18 mV between the bath and electrode solutions (estimated using the JPCalc programme [34]). The holding potential was 0 mV throughout. Compensation for cell capacitance and series resistance was made automatically by the EPC9 amplifier before each voltage ramp. As described in Section 3, in cells expressing hTRPC-1 maitotoxin initiated the activation of a large inward current which continued to increase in magnitude with increasing time after maitotoxin addition and, in some cases, led to cell death. For cells expressing hTRPC-1, the results presented include only those obtained with cells in which it was shown that the maitotoxin-initiated current could be effectively blocked by Gd^{3+}, Zn^{2+} or Cd^{2+}. For all patch-clamp recording data, unless otherwise specified, the results shown are the means ± S.E.M.

3. Results

3.1. Characterisation of maitotoxin-initiated divalent cation inflow in H4-IIE cells

In the presence of extracellular Ca^{2+}, a low concentration of maitotoxin (60 pM) caused a substantial increase in $[Ca^{2+}]_{cyt}$ (Fig. 1A) (cf. [7]). The onset of this effect was slow, taking about 4 min to achieve a maximal rate of increase in $[Ca^{2+}]_{cyt}$. The addition of maitotoxin to cells incubated in the absence of added extracellular Ca^{2+} caused no increase in $[Ca^{2+}]_{cyt}$ indicating that maitotoxin does not induce the release of Ca^{2+} from intracellular stores (Fig. 1B). This was further investigated by determining the amount of Ca^{2+} released by thapsigargin added 6 min after the addition of 300 pM maitotoxin to cells incubated in the absence of added Ca^{2+}. The thapsigargin-induced increase in $[Ca^{2+}]_{cyt}$ (peak height) was 0.063 ± 0.003 ($n = 7$) and 0.067 ± 0.002 ($n = 9$) fluorescence ratio units ($P > 0.05$) in the absence and presence of maitotoxin, respectively. Taken together, these results indicate that maitotoxin does not cause the release of a significant amount of Ca^{2+} from intracellular stores in H4-IIE cells.

The subsequent addition of extracellular Ca^{2+} to cells incubated in the presence of maitotoxin and absence of extracellular Ca^{2+} caused a large increase in $[Ca^{2+}]_{cyt}$ compared with the addition of Ca^{2+} in the absence of maitotoxin (Fig. 1B cf. A, and Table 2). Under the conditions employed (60–300 pM maitotoxin for 15 min), no obvious toxic effects of maitotoxin were observed, as assessed by the examination of cell morphology and the ability of the cells to retain fura-2. These results indicate that, as shown previously [7] for freshly isolated rat hepatocytes, maitotoxin initiates a significant increase in plasma membrane Ca^{2+} inflow in H4-IIE cells without causing a detectable release of Ca^{2+} from intracellular stores. Maitotoxin-stimulated Ca^{2+} inflow was inhibited by Gd^{3+} with half-maximal inhibition at approximately 1 μM Gd^{3+} (Fig. 2). Within the range of Gd^{3+} concentrations tested (0.5–10 μM) the inhibition by Gd^{3+} was not complete. Maitotoxin also

Table 2
Maitotoxin and thapsigargin initiate the activation of Ca^{2+} inflow in control H4-IIE cells and in cells expressing hTRPC-1

Cells	Agonist	Ca^{2+} inflow initiated by extracellular Ca^{2+} addition	
		Initial rate (nM/s)	Value of plateau following Ca^{2+}_o addition (nM)
Transfected with cDNA encoding EGFP alone	–	–	94 ± 4 (94 cells)
	Maitotoxin (60 pM)	2.87 ± 0.20 (109 cells)	699 ± 17 (109 cells)
	Thapsigargin (10 μM)	17.8 ± 0.6 (336 cells)	775 ± 22 (336 cells)
Co-transfected with cDNA encoding EGFP and hTRPC-1	–	–	92 ± 6 (97 cells)
	Maitotoxin (60 pM)	5.64 ± 0.61* (73 cells)	1117 ± 78* (73 cells)
	Thapsigargin (10 μM)	22.7 ± 0.7* (302 cells)	924 ± 11* (302 cells)

Cell transfection and the measurement of Ca^{2+} inflow were performed as described in Section 2 and in the legends of Figs. 1 and 8. Maitotoxin and thapsigargin, when present, were added before extracellular Ca^{2+} (5 mM). The values shown are the means ± S.E.M. for the total number of cells indicated and were obtained from 4–9 separate experiments. The degree of significance, determined using Student's *t*-test for unpaired samples, for a comparison of the values obtained for cells expressing hTRPC-1 with the corresponding value for control cells, is $*P < 0.05$. The degree of significance for a comparison of the values obtained in the presence of maitotoxin or thapsigargin with the corresponding value in the absence of agonist is $P < 0.01$.

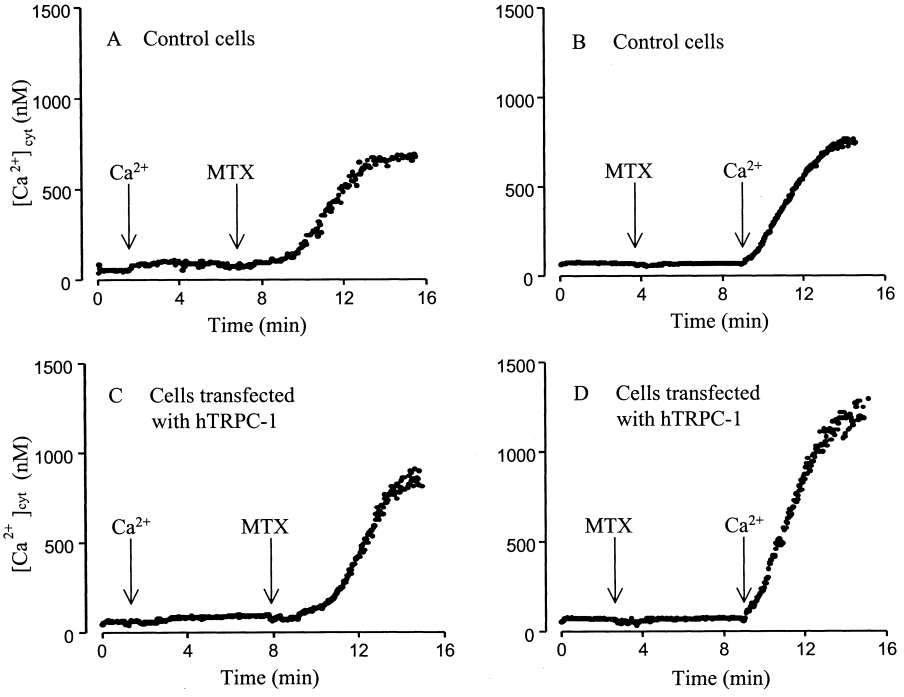

Fig. 1. Maitotoxin initiates the activation of Ca^{2+} inflow in control H4-IIE cells and in cells expressing hTRPC-1. (A,C) The effect of maitotoxin (MTX) added after extracellular Ca^{2+} to control cells (transfected with cDNA encoding EGFP) (A) or to cells co-transfected with cDNA encoding EGFP and hTRPC-1 (C). (B,D) The effect of maitotoxin added before the addition of extracellular Ca^{2+} to control cells (transfected with cDNA encoding EGFP) (B) or to cells co-transfected with cDNA encoding EGFP and hTRPC-1 (D). The times of addition of maitotoxin (MTX, 60 pM) and Ca^{2+} (5 mM) are indicated by the arrows. The traces shown are the means of those obtained from 17 (A), 20 (B), 19 (C) and 13 (D) cells in one experiment in each case, and are representative of the traces obtained in each of 4–9 separate experiments.

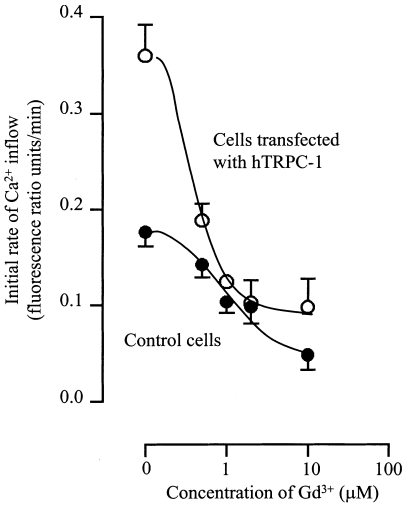

Fig. 2. Dose–response curves for the inhibition by Gd^{3+} of maitotoxin-initiated Ca^{2+} inflow (measured using fura-2) in control H4-IIE cells and in cells expressing hTRPC-1. Initial rates of Ca^{2+} inflow were measured in control cells (co-transfected with empty cDNA encoding EGFP and pcDNA3 vector) (closed circles) and in cells co-transfected with cDNA encoding EGFP and hTRPC-1 (open circles) in experiments similar to those shown in Fig. 1B,D as described in Section 2 using the HEPES-buffered saline medium. The results are the means ± S.E.M. (n = 3–6 independent experiments).

caused a substantial increase in the rate of Mn^{2+}-induced quenching of intracellular fura-2 when added 6 min before the addition of Mn^{2+} (Fig. 3 (control cells) and Table 3) (cf. [7]).

3.2. Detection of a maitotoxin-induced Na^+ current by patch-clamp recording

In whole cell patch-clamp recordings in which the pipette solution contained a strong Ca^{2+} buffer (10 mM EGTA) maitotoxin failed to induce any current (n = 9) within 10 min. When the pipette solution contained a weak Ca^{2+} buffer (1 mM EGTA and 1 mM Ca^{2+}), application of 60 pM maitotoxin in the external solution for 2–3 min activated an inward current (Fig. 4A). The average maximal amplitude at −100 mV was 320 ± 67 pA (n = 11). The reversal potential of the maitotoxin-activated current was about +10 mV and was not affected by varying the Cl^- concentration, indicating that the current activated by maitotoxin is a cation current. After reaching its maximal amplitude the maitotoxin-activated current declined slowly but could be repeatedly re-activated by the application of maitotoxin for 2–3-min periods.

The maitotoxin-induced current was blocked by

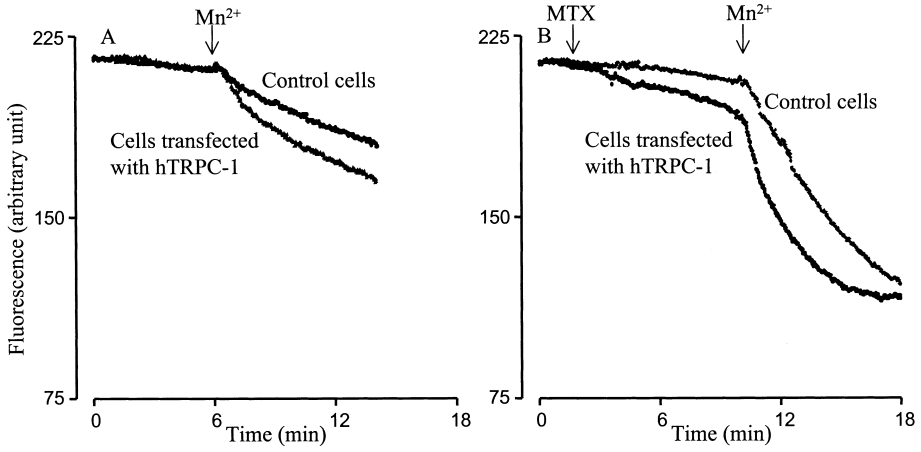

Fig. 3. Maitotoxin stimulates Mn^{2+} inflow in control H4-IIE cells and in cells expressing hTRPC-1. (A) The addition of Mn^{2+} in the absence of maitotoxin to control cells (transfected with cDNA encoding EGFP and empty pcDNA3 vector) (upper trace) and cells co-transfected with cDNA encoding EGFP and hTRPC-1 (lower trace). (B) The addition of Mn^{2+} following pre-treatment with maitotoxin (MTX) to control cells (transfected with cDNA encoding EGFP and empty vector) (upper trace) and cells co-transfected with EGFP and hTRPC-1 (lower trace). The times of addition of maitotoxin (MTX, 300 pM) and Mn^{2+} (100 μM) are indicated by the arrows. Mn^{2+} inflow was measured as described in Section 2 using the HEPES-buffered saline medium. The traces shown are the means of those obtained from 23 (A, control) and 17 (A, hTRPC-1), and 17 (B, control) and 22 (B, hTRPC-1) cells in one experiment in each case, and are representative of the traces obtained in each of five separate experiments.

Fig. 4. Maitotoxin initiates the activation of inward currents in control H4-IIE cells and in cells expressing hTRPC-1. (A) Time course of inward current development in control H4-IIE cells (co-transfected with cDNA encoding EGFP and empty pcDNA3 vector) after the addition of 60 pM maitotoxin (MTX) to the external solution, and inhibition of the current by Gd^{3+}. Each point on the trace represents the amplitude of the current at −100 mV taken from the current responses to the voltage ramps (−120 to +60 mV) applied every 2 s after establishing the whole cell configuration. The horizontal bars show the times of application of maitotoxin and solutions containing Gd^{3+}. The plot shown represents the results obtained for one of 15 cells which each gave similar results. (B) Instantaneous current–voltage relationship in the range −100 to +60 mV obtained for control cells in response to a voltage ramp at the time of maximal inward current development after maitotoxin addition to the control external solution, or where 140 mM extracellular Na^+ was replaced with 100 mM Ca^{2+}, or in control external solution in the presence of 10 μM Gd^{3+}. The plots shown represent the results obtained for one of seven cells which each gave similar results. (C) Time course of inward current development in H4-IIE cells expressing hTRPC-1 (co-transfected with cDNA encoding EGFP and hTRPC-1) after the addition of 60 pM maitotoxin (MTX) to the external solution, and inhibition of the current by Gd^{3+}. The plot shown represents the results obtained for one of nine cells which each gave similar results. Experimental details are as described in A. Note that the scale for the ordinate in C is much smaller than that for the ordinate in A. (D) Instantaneous current–voltage relationship in the range −100 to +60 mV obtained for cells expressing hTRPC-1 in response to a voltage ramp at the time of maximal inward current development after maitotoxin addition to the control external solution, or where 140 mM extracellular Na^+ was replaced with 100 mM Ca^{2+}, or in control external solution in the presence of 10 μM Gd^{3+}. The plots shown represent the results obtained for one of five cells which each gave similar results. (E) Amplitudes of the currents measured at −100 mV activated by maitotoxin in the control cells (co-transfected with cDNA encoding EGFP and empty pcDNA3 vector) ($n=11$) and in cells expressing hTRPC-1 (co-transfected with cDNA encoding EGFP and hTRPC-1) ($n=17$). (F) Dose-dependent inhibition of the maitotoxin-induced inward current by Gd^{3+} in the control cells transfected with empty pcDNA3 vector (open symbols) and cells expressing hTRPC-1 (filled symbols). The current amplitude at −100 mV obtained at various external Gd^{3+} concentrations was normalised to the control current obtained in the absence of Gd^{3+}. The results are the means ± S.E.M. Sigmoidal dose–response curves were fitted to the data with an offset, and a Hill coefficient of 1. The fit gave a K_d of 1.3 ± 0.1 μM ($n=4$) for control cells and 3.3 ± 0.2 μM ($n=4$) for cells expressing hTRPC-1.

→

concentrations of Gd^{3+} in the micromolar range with half-maximal inhibition at 1.3 ± 0.1 μM ($n=4$) (Fig. 4A,B,F). The block by 100 μM Gd^{3+} was not complete leaving a residual component of 10–30% of the initial amplitude of the current. This residual component was not affected by the replacement of Na^+ by $Tris^+$, suggesting that maitotoxin initiates the activation of both a Gd^{3+}-sensitive and a Gd^{3+}-insensitive NSCC or that the residual Gd^{3+}-insensitive component represents a non-specific leakage through the plasma membrane which has developed after the addition of maitotoxin. The Gd^{3+}-sensitive component of the maitotoxin-initiated current was also sensitive to the concentration of Ca^{2+} in the external solution. An increase in the Ca^{2+} concentration from 2 mM to 10 mM caused an approximately 50% reduction of the current amplitude (results not shown). At 100 mM external Ca^{2+} there was no detectable Gd^{3+}-sensitive current and the reversal potential of the residual current was shifted toward negative potentials (Fig. 4B). Moreover, in the presence of 100 mM extracellular Ca^{2+} the outward current was also reduced (Fig. 4B). These observations indicate that extracellular Ca^{2+} inhibits the maitotoxin-activated channel and suggest that, compared to Na^+, both Ca^{2+} conductance and Ca^{2+} permeability through the maitotoxin-activated channel are low.

3.3. Identification of mRNA encoding TRP proteins 1, 2 and 3 in H4-IIE cells and rat hepatocytes

Since it has been shown that TRP proteins, when expressed heterologously, form non-selective cation channels [26,35–37], experiments were directed towards identifying which of the TRP proteins 1–6 are expressed in liver cells, using RT–PCR as described in Section 2. PCR bands corresponding to the expected sizes of the amplified sequences for TRP proteins 1–6 were detected in rat brain mRNA, as shown previously [16,38] (Fig. 5 and Table 4). In mRNA from H4-IIE cells, the AML12 mouse liver cell line, and rat hepatocytes, PCR bands corresponding to the expected sizes of the amplified sequences for TRP proteins 1, 2 and 3, but not to TRP proteins 4, 5 and 6, were detected (Fig. 5 and Table 4). cDNA encoding the TRP-1 protein was detected with two separate primer sets, MTS 1/MTA (Fig. 5A) and MTS 2B/MTA (Fig. 5B), although the second was with reduced efficiency. The detection of cDNA encoding TRP-1 by the sec-

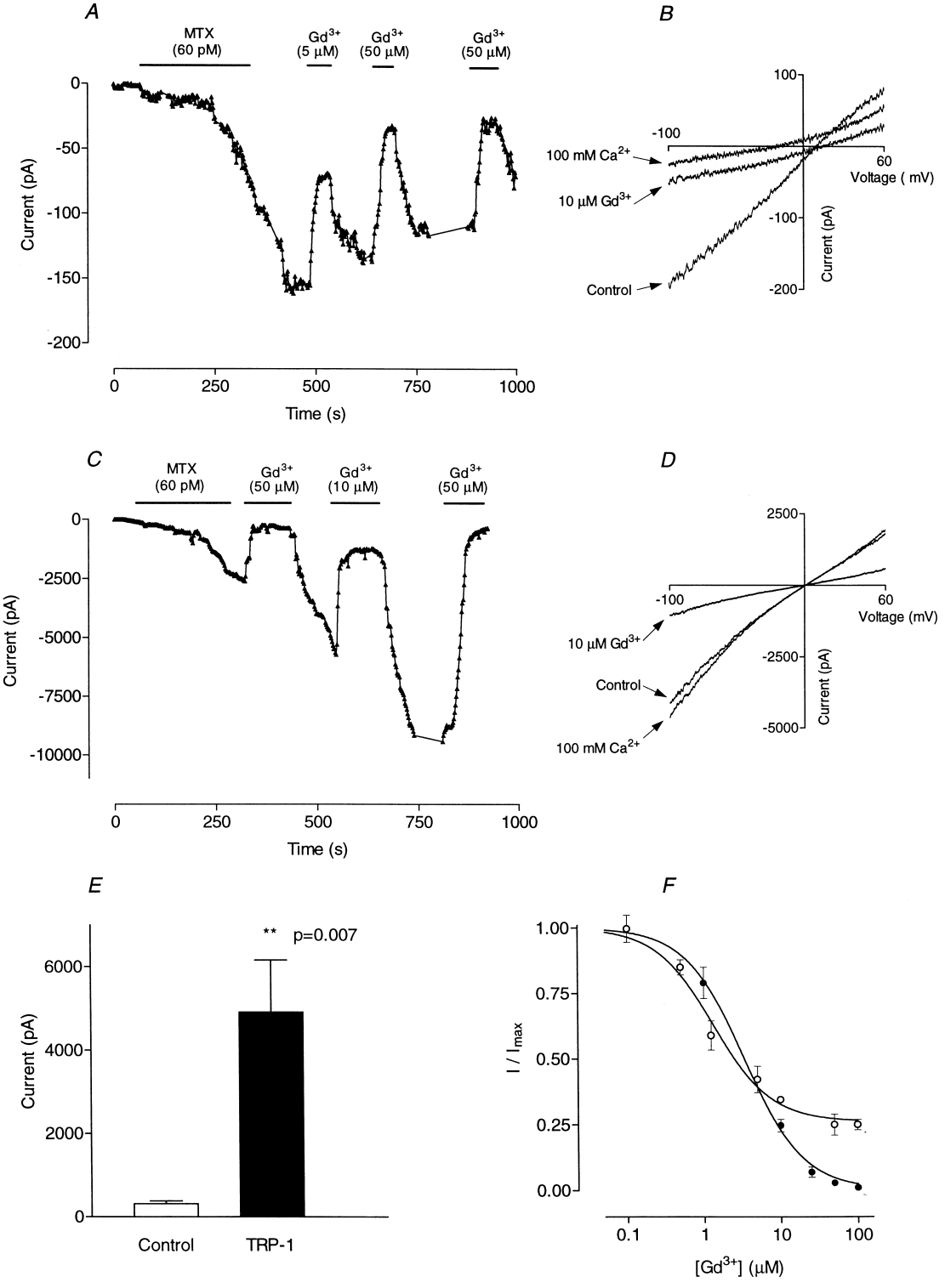
A
MTX
(60 pM)
Gd3+
(5 µM)
Gd3+
(50 µM)
Gd3+
(50 µM)
Current (pA)
0
-50
-100
-150
-200
0
250
500
750
1000
Time (s)
B
100
-100
100 mM Ca2+
60
Voltage (mV)
10 µM Gd3+
-100
Current (pA)
Control
-200
C
MTX
(60 pM)
Gd3+
(50 µM)
Gd3+
(10 µM)
Gd3+
(50 µM)
Current (pA)
0
-2500
-5000
-7500
-10000
0
250
500
750
1000
Time (s)
D
2500
-100
60
Voltage (mV)
10 µM Gd3+
Control
-2500
Current (pA)
100 mM Ca2+
-5000
E
** p=0.007
Current (pA)
6000
4000
2000
0
Control
TRP-1
F
1.00
0.75
0.50
0.25
0.00
I / Imax
0.1
1
10
100
[Gd3+] (µM)

Table 3
Maitotoxin initiates Mn^{2+} inflow in control H4-IIE cells and in cells expressing hTRPC-1

Cells	Rate of Mn^{2+} inflow (fluorescence units/min)		
	Basal	Maitotoxin present	Maitotoxin-stimulated rate
Co-transfected with cDNA encoding EGFP and empty pcDNA3 vector	6.1 ± 0.3 (119 cells)	12.9 ± 0.5 (97 cells)	6.7 ± 0.5 (5)
Co-transfected with cDNA encoding EGFP and hTRPC-1	10.7 ± 0.5 (92 cells)*	21.5 ± 1.3 (99 cells)**	10.8 ± 1.1 (5)*

Cell transfection and the measurement of Mn^{2+} inflow (in HEPES-buffered saline medium) were performed as described in Section 2 and in the legend of Fig. 3. The maitotoxin-stimulated rate of Mn^{2+} inflow was calculated for each separate experiment ($n = 5$) by subtracting the basal rate of Mn^{2+} inflow from that observed in the presence of maitotoxin. Maitotoxin, when present, was added 6 min before Mn^{2+} (100 μM). The values are the means ± S.E.M. for the total number of cells indicated and were obtained from five separate experiments. The degrees of significance, determined using Student's *t*-test for paired samples, for a comparison of the values obtained for cells expressing hTRPC-1 with the corresponding value for control cells are $*P \leq 0.05$ and $**P \leq 0.01$.

ond primer set is likely to be due to partial homology between MTS 2B and TRP-1 cDNA.

The abundance of the mRNA encoding TRP proteins 1, 2, and 3 in the liver cells compared with the abundance of the corresponding mRNA in rat brain was estimated using a strategy of limiting dilution PCR, using mRNA encoding glyceraldehyde 3-phosphate dehydrogenase as a reference. The abundance of TRP-1 mRNA was similar in all three liver cell types investigated, and similar to that in brain (Table 4). On the other hand, the abundance of TRP-2 in the liver cell lines was less than that in brain. The abundance of TRP-3 was more variable between the different liver cell types, and was lower than that in brain (Table 4).

Sequencing of the PCR products showed that the TRP-1, TRP-2 and TRP-3 fragments detected in rat liver are > 99% homologous (at the DNA level) with the corresponding rat TRP-1, -2 and -3 cDNA sequences in GenBank (accession numbers: AF061266 [39], AF136401 [40], AB022331 [41], respectively).

3.4. Heterologous expression of the hTRPC-1 protein in H4-IIE cells

In order to further test the idea that a TRP protein

Table 4
The size and limits of detection of the PCR products obtained by amplifying cDNA derived from mRNA encoding TRP proteins 1–6 in liver cells and rat brain

PCR primer	Highest dilution of cDNA from which PCR product was detected			
	H4-IIE cells	Rat hepatocytes	AML12 cells	Rat brain
TRP-1	1/10 000	1/10 000	1/10 000	1/10 000
TRP-2	1/10	1/5	1/10	1/33
TRP-3	1/10	1/33	1/33–1/100	1/100
TRP-4	No product	No product	No product	1/10
TRP-5	No product	No product	No product	1/33–1/100
TRP-6	No product	No product	No product	1/100
GAPDH	1/100 000	1/100 000	1/100 000	1/10 000–1/100 000

Values are the highest dilution of cDNA from which PCR product could be detected as a visible band by ethidium bromide staining in agarose gel after 45 cycles of amplification (GAPDH 35 cycles). The results were obtained from at least three amplifications from each of two (brain, AML12) or three (hepatocytes, H4-IIE) separate preparations of cDNA of each cell type. Where results were variable, a range of dilutions is given. Comparisons can be made horizontally between cell types, but not vertically between TRP types as the products were amplified using different primer sets. No bands were observed with any of the primer sets when reverse transcriptase was omitted from the reaction mixture for cDNA synthesis thus excluding the possibility that the PCR products were amplified from contaminating genomic DNA.

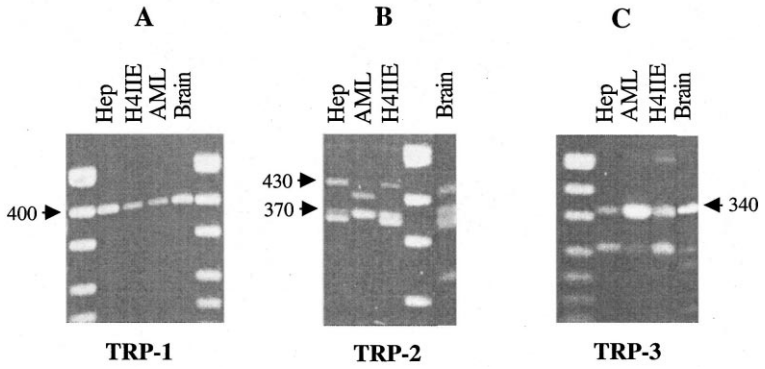

Fig. 5. PCR products amplified from mRNA isolated from H4-IIE cells, rat hepatocytes (Hep), the AML12 mouse liver cell line (AML) and rat brain using RT–PCR and primers corresponding to sequences of cDNA encoding TRP proteins 1, 2, and 3. The primers (Table 1) were: MTS 1/MTA, selective for TRP-1 (A); MTS 2B/MTA, selective for TRP-2, but also amplified TRP-1 (B); and MTS 3/MTA, selective for TRP-3 (C). The sizes of the PCR products are: 400 bp (A, TRP-1); 370 bp and 430 bp (B, TRP-2 and TRP-1, respectively); and 340 bp (C, TRP-3). Other bands in B and C were shown by DNA sequencing to be non-specific products unrelated to TRP. The unmarked lanes contain SPP1/*Eco*RI DNA size markers. The results shown are representative of those obtained in one of three similar experiments.

is the molecular correlate of the maitotoxin-initiated cation channel in H4-IIE cells, the hTRPC-1 protein was expressed in these cells. The predicted amino acid sequence of hTRPC-1 is 99% identical to that of rat TRP-1β [40]. This TRP protein was selected because, of the seven known animal cell TRP proteins, it is widely expressed in non-excitable animal cells [16]. H4-IIE cells were transiently co-transfected with cDNA encoding EGFP and hTRPC-1, and GFP fluorescence used to assess transfection efficiencies and to identify individual transfected cells. From the proportion of cells expressing EGFP, the efficiency of the transient transfection was estimated to be about 5–10%. The degree of expression of the hTRPC-1 protein in a population of co-transfected H4-IIE cells was assessed using Western blot analysis. In cell extracts, a band with an apparent molecular mass of about 80 kDa, which was not present in extracts of control cells, was observed using a polyclonal antibody raised against a peptide corresponding to the 18 amino acids at the carboxy terminus of TRP-1 (Fig. 6A, lane 2 cf. lane 1). Appearance of this 80 kDa band was prevented when the anti-TRP-1 antibody was blocked with the antigenic peptide (Fig. 6A, lane 4 cf. lane 2). Analysis of proteins extracted from H4-IIE cells expressing hTRPC-1 at several time points after transient transfection showed that the intensity of the 80 kDa band, but not that of the other bands, increased to a maximum at about 24 h, then declined (Fig. 6B,C).

The size (80 kDa) of the hTRPC-1 protein expressed in H4-IIE cells is smaller than the predicted size (87 kDa) [17] for hTRPC-1 and the estimated size (92 kDa) of the band attributed to the expressed hTRP-1 protein in extracts of COS cells transfected with DNA encoding hTRP-1 [40]. However, it corresponds to the observed size (80 kDa) of TRPC-1 expressed in insect Sf9 cells [35] and hTRPC-1 expressed in *Xenopus* oocytes [28], and endogenous TRP-1 in *Xenopus* oocytes [28]. Bands of 100, 110 and approximately 200 kDa were also detected in both control and co-transfected H4-IIE cells (Fig. 6A, lanes 1 and 2). These may represent proteins which contain epitopes which bind the anti-TRP-1 antibody but are not components of the TRP-1 protein.

Examination of the intracellular location of expressed hTRPC-1 showed that most of the expressed protein is located in interior regions of the cell. Fig. 7A,B show a field of 11 cells of which three exhibited EGFP fluorescence (Fig. 7A) and hTRPC-1 immunofluorescence (Fig. 7B). A control image in which the anti-hTRPC-1 antibody was replaced by pre-immune serum is shown in Fig. 7C. Most of the expressed hTRPC-1 protein appears to be located in the ER and the Golgi networks, some at the plasma membrane, and none in the nucleus (Fig. 7B). In order to determine whether the majority of the hTRPC-1 protein is present in cellular membranes, subcellular fractionation and Western blot analysis

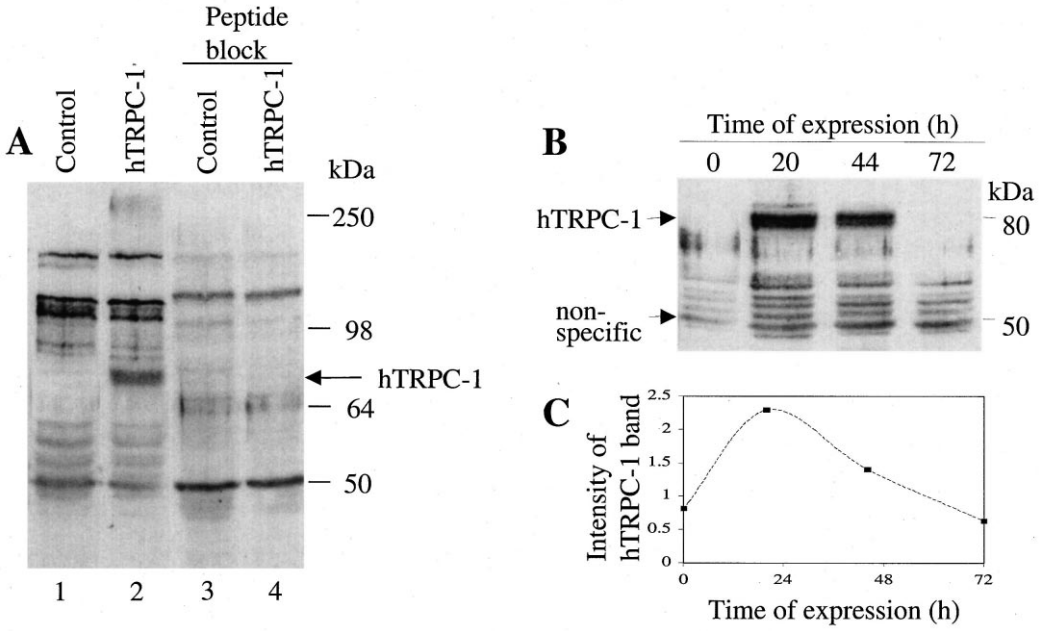

Fig. 6. The detection by Western blot analysis of the expressed hTRPC-1 protein in H4-IIE cells transfected with cDNA encoding hTRPC-1. (A) Proteins extracted from cells co-transfected with cDNA encoding EGFP and hTRPC-1 and control cells (transfected with cDNA encoding EGFP). For the two lanes marked 'peptide block', the anti-TRP-1 antibody was pre-incubated with blocking peptide as described in Section 2. (B) Proteins extracted from H4-IIE cells expressing hTRPC-1 at different times after co-transfection of the cells with cDNA encoding EGFP and hTRPC-1. The times elapsed (h) after cell transfection are indicated for each lane. (C) A plot of the relative intensity of the 80 kDa hTRPC-1 band in B as a function of time. The intensity of the 80 kDa band is expressed as a ratio of the intensity of the 50 kDa band (indicated by the arrow in B) in order to take into account variations in the amounts of protein applied to the gel and transferred from the gel to the membrane. The results shown are those obtained for each of 10 (A, lanes 1 and 2), 2 (A, lanes 3 and 4), and 2 (B,C) experiments which each gave similar results.

were conducted. The results indicate that all the expressed hTRPC-1 protein is located in cellular membranes (Fig. 7D).

The detection of hTRPC-1 by immunofluorescence was also used to estimate the extent of hTRPC-1 expression as a function of time after transient transfection of the cells. At 24 h after co-transfection with cDNA encoding EGFP and hTRPC-1 about 40% of the cells which exhibited EGFP fluorescence also expressed the hTRPC-1 protein. At 48 h, the number of cells expressing hTRPC-1 had decreased to about 20% of the cells which expressed EGFP.

3.5. *Enhancement of maitotoxin-initiated Ca^{2+} and Mn^{2+} inflow in H4-IIE cells heterologously expressing hTRPC-1*

Maitotoxin-initiated Ca^{2+} inflow was greatly enhanced in cells expressing hTRPC-1 (Fig. 1D cf. B, and Table 2). In the Ca^{2+} add-back protocol, the initial rate of Ca^{2+} inflow and the magnitude of the subsequent plateau of $[Ca^{2+}]_{cyt}$ were enhanced by about 100% and 60%, respectively, in cells expressing hTRPC-1. hTRPC-1 expression did not detectably enhance Ca^{2+} inflow in the absence of maitotoxin (Fig. 1C cf. A, and Table 2). When maitotoxin was added to cells initially incubated in the presence of extracellular Ca^{2+}, the maitotoxin-induced plateau of $[Ca^{2+}]_{cyt}$ was increased by 60% in cells expressing hTRPC-1 compared with control cells (Fig. 1C cf. A). The value of the plateau reached after maitotoxin addition was 440 ± 23 (94 cells) and 921 ± 16 (97 cells) nM ($P \leq 0.05$, unpaired t-test) for control cells (transfected with EGFP) and cells transfected with hTRPC-1, respectively. The dose–response curve for the inhibition by Gd^{3+} of maitotoxin-induced Ca^{2+} inflow in cells expressing hTRPC-1 was determined and compared with that for non-transfected cells (Fig. 2). In cells transfected with hTRPC-1, the con-

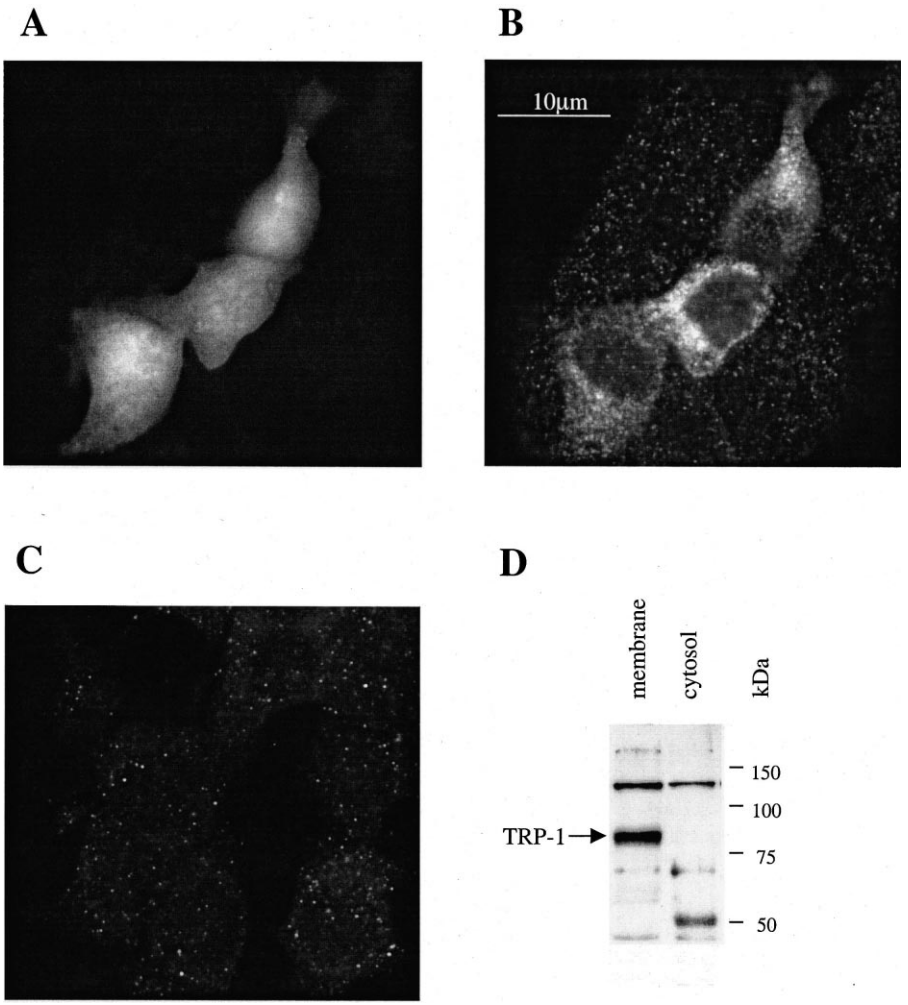

Fig. 7. Intracellular location of the expressed hTRPC-1 protein in H4-IIE cells. (A) A high-resolution fluorescence microscope image of a field of 11 cells co-transfected with cDNA encoding EGFP and hTRPC-1 showing three cells expressing EGFP. (B) Image of the same field of cells as in A showing Cy3 fluorescence (indicating the expression of hTRPC-1) for the three cells in A which exhibit GFP fluorescence. (C) Image of Cy3 fluorescence of a field of cells co-transfected with cDNA encoding EGFP and hTRPC-1 under conditions where the anti-TRP-1 antibody was replaced by pre-immune rabbit serum. The results shown in A–C are representative of those obtained in three separate transient transfection experiments. Scale bar = 10 μm. (D) Western blot analysis of a membrane and a cytosolic fraction from cells expressing hTRPC-1. Preparation of the membrane and cytosolic fractions and Western blot analysis were conducted as described in Section 2. The results shown are those obtained from one of two Western blots performed on membrane fractions from one transient transfection experiment.

centration of Gd^{3+} which gave half-maximal inhibition was approximately 1 μM which is comparable with that obtained for control cells (transfected with empty vector). As observed for control cells, inhibition of maitotoxin-initiated Ca^{2+} inflow in cells expressing hTRPC-1 was not complete.

Cells expressing hTRPC-1 exhibited a 70% enhancement of basal Mn^{2+} inflow (Fig. 3A and Table 3) and a 60% enhancement of maitotoxin-stimulated Mn^{2+} inflow (Fig. 3B cf. A, and Table 3). hTRPC-1 expression also enhanced thapsigargin-stimulated Ca^{2+} inflow by about 20% (Fig. 8 and Table 2) but did not affect thapsigargin-induced release of Ca^{2+} from intracellular stores.

3.6. *Analysis of cells expressing hTRPC-1 by patch-clamp recording*

In cells transfected with hTRPC-1 and with weak Ca^{2+} buffer in the pipette, maitotoxin (60 pM) acti-

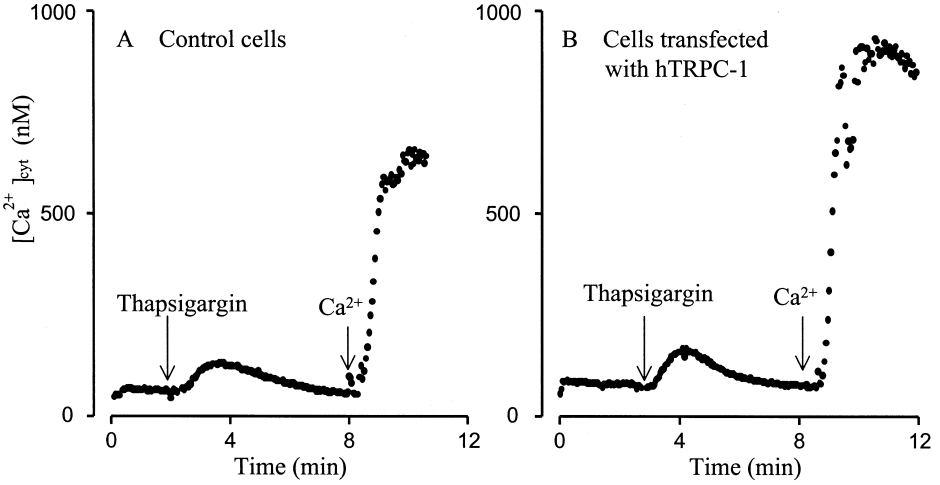

Fig. 8. Thapsigargin initiates the activation of Ca^{2+} inflow in H4-IIE cells expressing hTRPC-1. The times of addition of thapsigargin (10 μM) and Ca^{2+} (5 mM) to control cells (transfected with cDNA encoding EGFP) and cells co-transfected with cDNA encoding EGFP and hTRPC-1 are shown by the arrows. The traces shown are the means of those obtained from 24 (A) and 44 (B) cells in one experiment in each case, and are representative of the traces obtained in each of nine separate experiments.

vated a significantly larger cation current than that observed in non-transfected cells (Fig. 4C cf. A, and Fig. 4E). (The current amplitude scale for Fig. 4C is much smaller than that for Fig. 4A) In the absence of maitotoxin, no current was detected over a time period of 1000 s. Moreover, no maitotoxin-activated current was observed in cells transfected with hTRPC-1 with the strong Ca^{2+} buffer in the pipette. When the maitotoxin was washed out, the amplitude of the current in hTRPC-1 transfected cells kept increasing (Fig. 4C), frequently resulting in the cell death. The maitotoxin-initiated current in hTRPC-1-transfected cells was blocked by Gd^{3+} with half-maximal inhibition at 3.4 ± 0.3 μM ($n = 4$; Fig. 4C,D,F). The current was also partially blocked by Zn^{2+} and Cd^{2+} in the range 1–10 mM (results not shown). The average maximal amplitude of the maitotoxin-initiated current in hTRPC-1 transfected cells was 4.9 ± 1.3 nA ($n = 11$) at −100 mV. When the external solution contained 100 mM Ca^{2+}, the current–voltage plot was identical to that obtained using normal external solution (140 mM Na^+) (Fig. 4D). Thus, unlike the cation channels activated by maitotoxin in non-transfected cells, channels in hTRPC-1 transfected cells showed no block by extracellular Ca^{2+} and the same permeability for Ca^{2+} as for Na^+. Application of the external solution which contained 100 mM Ca^{2+} for more than 2 min resulted in a further increase of the current amplitude to values that could not be properly clamped by the amplifier (results not shown).

TRP-1 is considered to be one of the candidates for a store operated Ca^{2+} channel [37,42–44]. It has previously been shown, using patch-clamp recording, that H4-IIE cells possess store-operated Ca^{2+} channels which have a very high selectivity for Ca^{2+} compared with Na^+ and are indistinguishable from the Ca^{2+} release-activated Ca^{2+} channels (CRAC channels) well characterised in lymphocytes and mast cells [2]. The possibility that hTRPC-1 is a store-operated Ca^{2+} channel in H4-IIE cells was investigated by depleting internal Ca^{2+} stores using a strong Ca^{2+} buffer pipette solution. In hTRPC-1 transfected cells, this resulted in activation of a Ca^{2+}-selective current which was identical in magnitude to the store-operated Ca^{2+} current (I_{CRAC}) observed previously in non-transfected H4-IIE cells [2] ($n = 8$, results not shown). There was no evidence for the activation of any other type of store-operated Ca^{2+} channel in cells transfected with hTRPC-1.

4. Discussion

4.1. Characteristics of the maitotoxin-activated endogenous cation channel in H4-IIE cells

The results obtained using fura-2 and patch-clamp

recording indicate that maitotoxin initiates the activation of a cation channel which admits Na^+, Ca^{2+} and Mn^{2+}; has a high selectivity for Na^+ compared with Ca^{2+}; is inhibited when the extracellular Ca^{2+} concentration is increased; and is inhibited by Gd^{3+} at concentrations in the micromolar range. The observation that channels are not activated when the cytoplasmic space is perfused with a strong Ca^{2+} buffer (10 mM EGTA) indicates that the process by which the channel is activated requires at least a basal level of $[Ca^{2+}]_{cyt}$. These properties, together with knowledge of the mechanism of action of maitotoxin on cells [7–13] and the absence of evidence for maitotoxin-induced cell toxicity and cell lysis (cf. results obtained for some other cell types [8]) suggest that the maitotoxin-activated NSCCs are endogenous liver cell channels.

The likely steps (cf. [7–13]) in the process by which maitotoxin activates NSCCs in H4-IIE cells are: the binding of the toxin to a specific protein on the plasma membrane [13] or possibly insertion of the hydrophobic polycyclic ether moieties of the toxin into the plasma membrane to create a non-specific pore which admits Na^+ and Ca^{2+} and other cations; increases in the intracellular concentrations of Na^+ and Ca^{2+}; activation of endogenous NSCCs; and inflow of Na^+ and Ca^{2+} through endogenous NSCCs. The toxin may activate both a Gd^{3+}-sensitive and a Gd^{3+}-insensitive NSCC. Alternatively, Gd^{3+}-insensitive component of maitotoxin-stimulated Ca^{2+} and Na^+ inflow may represent movement of the cations through the pore formed by maitotoxin itself whereas the Gd^{3+}-sensitive component most likely represents endogenous maitotoxin-activated NSCCs. It is considered unlikely that the process by which maitotoxin activates Ca^{2+} and Na^+ inflow in H4-IIE cells involves the release of Ca^{2+} from the endoplasmic reticulum (cf. results reported by others for fibroblasts [8,45]) since no evidence was obtained in the present experiments to indicate that maitotoxin induces Ca^{2+} release from intracellular stores. A noticeable feature of the action of maitotoxin is the relatively slow time of onset for the activation of Ca^{2+} inflow (cf. [7]). This may be due to a slow accumulation of the toxin in the plasma membrane and/or to the insertion of endogenous NSCC proteins into the plasma membrane (cf. [9]).

Several properties of the maitotoxin-activated NSCC, including the block by extracellular Ca^{2+}, high permeability for Na^+, permeability to Mn^{2+} as well as Ca^{2+}, and inhibition of Na^+ inflow when the extracellular Ca^{2+} concentration is increased are similar to properties reported for mast cell receptor-activated NSCCs [46]. These channels can be activated by agonists and the secretagogue 48/80, have a conductance of 50 pS, principally admit Na^+ but can also admit Ca^{2+} and Mn^{2+}, are inhibited by protein kinase C and by the movement of Ca^{2+} through the channel, and play a role (in conjunction with store-operated Ca^{2+} channels) in regulating $[Ca^{2+}]_{cyt}$ [46].

4.2. Endogenous TRP proteins expressed in liver cells

The results of the RT–PCR experiments indicate that mRNA encoding TRP proteins 1, 2 and 3 is expressed in freshly isolated rat hepatocytes, a rat liver cell line (H4-IIE) and a mouse liver cell line (AML12). The results obtained using limiting dilution PCR indicate that the level of expression of TRP-1 mRNA in liver cells is comparable with that in brain. The inability to detect the endogenous TRP-1 protein by Western blot or immunofluorescence is most likely due to a relatively low affinity of the anti-TRP-1 antibody employed for the TRP-1 protein (T.K. Chataway, H. Brereton, G.J. Barritt, unpublished results). The conclusion that TRP proteins 1 and 3 are expressed in liver cells is consistent with the observations of others who have reported the detection of mRNA encoding the TRP-1 [17,38,39,47,48] and TRP-3 [38] proteins in liver using RT–PCR or Northern blot analysis, and detection of the TRP-1 protein in *Xenopus* oocyte liver [48].

4.3. Characteristics of the maitotoxin-activated cation inflow through the heterologously expressed hTRPC-1 protein

The immunofluorescence and Western blot results obtained with H4-IIE cells heterologously expressing hTRPC-1 indicate that, while some of the expressed protein is located at the plasma membrane, a considerable amount is located in intracellular membranes. Further evidence for the location of some expressed hTRPC-1 in the plasma membrane is provided by

results of the patch-clamp recording experiments which clearly demonstrate the appearance of a new type of current in cells expressing hTRPC-1. Correlation of the immunofluorescence results (present study) with the intracellular location of the endoplasmic reticulum in H4-IIE cells [3] suggests that considerable amounts of hTRPC-1 are located in the endoplasmic reticulum and Golgi networks. Similar observations of an intracellular location of heterologously expressed TRP-1 have been made by others with other cell types [37,40]. Expressed hTRPC-1 may accumulate in the endoplasmic reticulum and Golgi because the cells are synthesising amounts of the hTRPC-1 protein which are well in excess of the quantities normally processed and trafficked to the plasma membrane (cf. regulation of the translocation from intracellular compartments to the plasma membrane of growth factor-regulated channel (a member of the TRP family of proteins) induced by insulin-like growth factor-1 [49], and K^+ channels expressed in *Xenopus* oocytes [50]). Three other explanations for the presence of expressed hTRPC-1 in the endoplasmic reticulum and Golgi are (i) recycling of plasma membrane hTRPC-1 back to the endoplasmic reticulum via endosomes and endocytosis, (ii) mistargeting of the hTRPC-1 protein in the environment of the liver cell (a highly polarised epithelial cell in which mechanisms which ensure the correct targeting of plasma membrane proteins are complex [51,52]), and (iii) the possibility that endogenous TRP-1 and heterologously expressed hTRPC-1 are located at the endoplasmic reticulum so that they can exert a physiological function at this site. At present, these possible explanations cannot be eliminated.

The heterologous expression of hTRPC-1 caused an enhancement of maitotoxin-initiated Ca^{2+} and Mn^{2+} inflow and the appearance of a large maitotoxin-initiated current with properties which differ from those of the maitotoxin-initiated current observed in control cells. The maitotoxin-activated channel in cells expressing hTRPC-1 is characterised by an approximately equal permeability to Ca^{2+} and Na^+ and inhibition by Gd^{3+} (half-maximal inhibition at 3 μM Gd^{3+}). These properties are similar to those reported by others for TRP-1 heterologously expressed in other cell types [35,36,38]. Since the appearance of this current was dependent on expression of hTRPC-1 it can be concluded that it is mediated by the presence of hTRPC-1 polypeptides in the plasma membrane either as a homo- or hetero-tetramer (e.g. composed of hTRPC-1 and one or more endogenous channel-forming polypeptides). Another possibility which cannot be excluded is that expression of hTRPC-1 induces the 'upregulation' or activation of an endogenous channel which is not otherwise activated by maitotoxin.

If maitotoxin can initiate the activation of expressed hTRPC-1, and control H4-IIE cells express the endogenous TRP-1 protein, it would be expected that maitotoxin could also activate endogenous TRP-1 leading to the appearance of a current with the characteristics of the hTRPC-1 current in control cells. The failure to detect such a current in control cells may be because (i) the amount of endogenous TRP-1 protein is low and hence the associated current is masked by the endogenous maitotoxin-activated NSCC current, and/or (ii) the endogenous TRP-1 polypeptides form heterotetramers with other channel-forming peptides to yield a channel with properties which differ from those of hTRPC-1 homotetramers which may form when hTRPC-1 is over-expressed.

The observations that the maitotoxin-initiated inward current observed in cells expressing hTRPC-1 does not develop when the cells are perfused with a strong intracellular Ca^{2+} buffer and increases dramatically when 100 mM Ca^{2+} is present in the extracellular medium for a prolonged period of time suggest that, in the environment of H4-IIE cells, expressed hTRPC-1 is activated by an increase in $[Ca^{2+}]_{cyt}$. Although initiation of the activation of the hTRPC-1 channel depends on the presence of maitotoxin, further activation occurred in the absence of the toxin. Such an 'autocatalytic' activation could be due to the effect of an increase in $[Ca^{2+}]_{cyt}$ on a Ca^{2+}-activated hTRPC-1 channel or a maitotoxin-induced insertion of hTRPC-1 polypeptides into the plasma membrane (cf. the suggestion that maitotoxin induces the insertion of cation channels into the *Xenopus* oocyte plasma membrane [9]).

Recently it has been shown using patch-clamp recording that H4-IIE cells possess a highly Ca^{2+}-selective store-operated Ca^{2+} channel which is indistinguishable from the Ca^{2+} release-activated Ca^{2+} channels (CRAC channels) in lymphocytes and mast cells [2]. Moreover, studies which have em-

ployed 2-aminoethyl phenylborate (2-APB) as an inhibitor of store-operated Ca^{2+} channels suggest that CRAC-like channels are the predominant store-operated Ca^{2+} channel in H4-IIE cells [53]. In the present study, no evidence was obtained to indicate that hTRPC-1 expression enhances the inward current due to Ca^{2+} inflow through the CRAC-like channels in H4-IIE cells. Moreover, the cation specificity of the hepatocyte store-operated Ca^{2+} channel [2] is very different from that of the hTRPC-1 channel (present results). Thus it can be concluded that hTRPC-1 is unlikely to be the major liver cell store-operated Ca^{2+} channel.

On the basis of differences in cation specificity and susceptibility to inhibition by Gd^{3+} of the endogenous maitotoxin-activated NSCC and the expressed hTRPC-1 protein, it is concluded that it is unlikely that the endogenous TRP-1 protein is the molecular counterpart of the maitotoxin-activated endogenous NSCC in H4-IIE cells. Further experiments are required to elucidate the functions of the TRP-1 protein and the TRP-2 and -3 proteins in liver cells. Their functions may include the regulation of liver cell volume and shape (cf. [5]). Experiments directed towards elucidation of the functions of TRP-1 will be aided by the observation that maitotoxin is an effective initiator of hTRPC-1 channel activation.

Acknowledgements

We thank Diana Tanevski for preparing the typescript, Mike Calder for excellent technical assistance, and Dr Peter Kolesik, Department of Horticulture, Viticulture and Oenology, University of Adelaide, for advice and assistance with confocal microscopy. This work was supported by a grant from the Australian Research Council.

References

[1] G.J. Barritt, in: R. Pochet, R. Donato, J. Haiech, C. Heizmann, V. Gerke (Eds.), Calcium: The Molecular Basis of Calcium Action in Biology and Medicine, Kluwer Academic Publishers, Dordrecht, 2000, pp. 73–94.
[2] G. Rychkov, H.M. Brereton, M.L. Harland, G.J. Barritt, Hepatology 33 (2001) 938–947.
[3] A. Auld, J. Chen, H.M. Brereton, Y.-J. Wang, R.B. Gregory, G.J. Barritt, Biochim. Biophys. Acta 1497 (2000) 11–26.
[4] S.D. Lidofsky, A. Sostman, J.G. Fitz, J. Membr. Biol. 157 (1997) 231–236.
[5] J. Graf, D. Häussinger, J. Hepatol. 24 (1996) 53–77.
[6] G.J. Barritt, Biochem. J. 337 (1999) 153–169.
[7] N.M. Woods, C.J. Dixon, T. Yasumoto, K.S.R. Cuthbertson, P.H. Cobbold, Cell. Signal. 11 (1999) 805–811.
[8] W.P. Schilling, W.G. Sinkins, M. Estacion, Am. J. Physiol. 277 (1999) C755–C765.
[9] W.-M. Weber, C. Popp, W. Clauss, W. van Driessche, Pflügers Arch. Eur. J. Physiol. 439 (2000) 363–369.
[10] I.F. Musgrave, R. Seifert, G. Schultz, Biochem. J. 301 (1994) 437–441.
[11] M. Murata, T. Yasumoto, Nat. Prod. Rep. 17 (2000) 293–314.
[12] L.I. Escobar, C. Salvador, M. Martinez, L. Vaca, Neurobiology 6 (1998) 59–74.
[13] D. Gutierrez, L. Diaz de Leon, L. Vaca, Cell Calcium 22 (1997) 31–38.
[14] R. Nath, M. Davis, A.W. Probert, N.C. Kupina, X. Ren, G.P. Schielke, K.K.W. Wang, Biochem. Biophys. Res. Commun. 274 (2000) 16–21.
[15] T. Hofmann, M. Schaefer, G. Schultz, T. Gudermann, J. Mol. Med. 78 (2000) 14–25.
[16] C. Harteneck, T.D. Plant, G. Schultz, Trends Neurosci. 23 (2000) 159–166.
[17] P.D. Wes, J. Chevesich, A. Jeromin, C. Rosenberg, G. Stetten, C. Montell, Proc. Natl. Acad. Sci. USA 92 (1995) 9652–9656.
[18] H.M. Brereton, M.L. Harland, M. Froscio, T. Petronijevic, G.J. Barritt, Cell Calcium 22 (1997) 39–52.
[19] J.C. Wu, G. Merlino, N. Fausto, Proc. Natl. Acad. Sci. USA 91 (1994) 674–678.
[20] K.S. Jakobsen, M. Haugen, S. Saeboe-Larssen, K. Hollung, M. Espelund, E. Hornes, in: M. Uhlen, E. Hornes, O. Olsvik (Eds.), Advances in Biomagnetic Separation, Eaton Publishing, Natick, MA, 1994, pp. 61–71.
[21] J. Sambrook, E.F. Fritsch, T. Maniatis, Molecular Cloning: A Laboratory Manual, 2nd Edition, Cold Spring Harbor Laboratory Press, Cold Spring Harbor, NY, 1989, pp. 7.43–7.52.
[22] C. Montell, G.M. Rubin, Neuron 2 (1989) 1313–1323.
[23] A.M. Phillips, A. Bull, L.E. Kelly, Neuron 8 (1992) 631–642.
[24] X. Zhu, P.B. Chu, M. Peyton, L. Birnbaumer, FEBS Lett. 37 (1995) 193–198.
[25] C.C.H. Petersen, M.J. Berridge, M.F. Borgese, D.L. Bennett, Biochem. J. 331 (1995) 41–44.
[26] X. Zhu, M. Jiang, M. Peyton, G. Boulay, R. Hurst, E. Stefani, L. Birnbaumer, Cell 85 (1996) 661–671.
[27] J.Y. Tso, X.-H. Sun, T.H. Kao, K.S. Reece, R. Wu, Nucleic Acids Res. 13 (1985) 2485–2502.
[28] H.M. Brereton, M.L. Harland, A.M. Auld, G.J. Barritt, Mol. Cell. Biochem. 214 (2000) 63–74.
[29] M.M. Bradford, Anal. Biochem. 72 (1976) 248–254.
[30] E. Harlow, D. Lane, Antibodies: A Laboratory Manual,

Cold Spring Harbor Laboratory Press, Cold Spring Harbor, NY, 1998.
[31] H.J. Xu, K. Umapathysivam, J. McNeilage, T.P. Gordon, P.J. Roberts-Thompson, J. Immunol. Methods 146 (1992) 241–247.
[32] A. Thomas, F. Delaville, in: J.G. McCormack, P.H. Cobbold (Eds.), Cellular Calcium: A Practical Approach, Oxford University Press, New York, 1991, pp. 1–54.
[33] O.P. Hamill, A. Marty, E. Neher, B. Sakmann, F.J. Sigworth, Pflügers Arch. 391 (1981) 85–100.
[34] P.H. Barry, J. Neurosci. Methods 51 (1994) 107–116.
[35] W.G. Sinkins, M. Estacion, W.P. Schilling, Biochem. J. 331 (1998) 331–339.
[36] C. Zitt, A. Zobel, A.G. Obukhov, C. Harteneck, F. Kalkbrenner, A. Lückoff, G. Schultz, Neuron 16 (1996) 1189–1196.
[37] X. Liu, W. Wang, B.B. Singh, T. Lockwich, J. Jadlowiec, B. O'Connell, R. Wellner, M.X. Zhu, I.S. Ambudkar, J. Biol. Chem. 275 (2000) 3403–3411.
[38] R.L. Garcia, W.P. Schilling, Biochem. Biophys. Res. Commun. 239 (1997) 279–283.
[39] W. Wang, B. O'Connell, R. Dykeman, T. Sakai, C. Delporte, W. Swaim, X. Zhu, L. Birnbaumer, I.S. Ambudkar, Am. J. Physiol. 276 (1999) C969–C979.
[40] E.R. Liman, D.P. Corey, C. Dulac, Proc. Natl. Acad. Sci. USA 96 (1999) 5791–5796.
[41] G. Ohki, T. Miyoshi, M. Murata, K. Ishibashi, M. Imai, M. Suzuki, J. Biol. Chem. 275 (2000) 39055–39060.
[42] T.P. Lockwich, X. Liu, B.B. Singh, J. Jadlowiec, S. Weiland, I.S. Ambudkar, J. Biol. Chem. 275 (2000) 11934–11942.
[43] X. Wu, G. Babnigg, M.L. Villereal, Am. J. Physiol. Cell Physiol. 278 (2000) C526–C536.
[44] J.A. Rosado, S.O. Sage, Biochem. J. 350 (2000) 631–635.
[45] D. Gutierrez, L.O. de Leon, L. Vaca, Cell Calcium 22 (1997) 31–38.
[46] C. Fasolato, M. Hoth, G. Matthews, R. Penner, Proc. Natl. Acad. Sci. USA 90 (1993) 3068–3072.
[47] H. Sakura, F.M. Ashcroft, Diabetologia 40 (1997) 528–532.
[48] L.K. Bobanovic, M. Laine, C.C.H. Petersen, D.L. Bennett, M.J. Berridge, P. Lipp, S.J. Ripley, M.D. Bootman, Biochem. J. 340 (1999) 593–599.
[49] M. Kanzaki, Y.-Q. Zhang, H. Mashima, L. Li, H. Shibata, I. Kojima, Nat. Cell Biol. 1 (1999) 165–170.
[50] D. Ma, N. Zerangue, Y.-F. Lin, A. Collins, M. Yu, Y.N. Jan, L.Y. Jan, Science 291 (2001) 316–319.
[51] V. Bender, S. Büschlen, D. Cassio, J. Cell Sci. 111 (1998) 3437–3450.
[52] J.A. Dranoff, M. McClure, A.D. Burgstahler, L.A. Denson, A.R. Crawford, J.M. Crawford, S.J. Karpen, M.H. Nathanson, Hepatology 30 (1999) 223–229.
[53] R.B. Gregory, G. Rychkov, G.J. Barritt, Biochem. J. 354 (2001) 285–290.